Full Wave Modeling of Conducting Posts in Rectangular Waveguides and Its Applications to Slot Coupled Combline Filters

Hui-Wen Yao, *Student Member, IEEE*, Kawthar A. Zaki, *Fellow, IEEE*, Ali E. Atia, *Fellow, IEEE*, and Rafi Hershtig

***Abstract*—A full wave model of conducting posts in rectangular waveguides yielding their generalized S-matrix is presented. By cascading the generalized scattering matrices of the posts and waveguide discontinuities, slot couplings between two combline resonators are obtained. The validation and accuracy of the method are confirmed by comparing the numerical results with measured data. It is shown that both electric and magnetic couplings can be obtained by changing the slot positions, and the electric coupling is more sensitive to the tuning screw than magnetic coupling. A 6-pole slot coupled combline filter with asymmetrical transmission zeros is designed and built. Excellent filter responses are obtained.**

I. Introduction

WITH RAPID DEVELOPMENT of mobile communications, the requirement for compact, low-cost, and high performance filters is increasing. One class of filters with these merits is combline filters. The conventional combline filter consists of a set of metal bars, properly spaced, grounded at one end and loaded by lumped capacitors or open circuit at the other side [1]. The synthesis and design procedures for this kind of filters were studied intensively [1]–[6]. The comblines are viewed as coupled TEM mode transmission lines.

In some cases, for instance, in design of a combline filter with narrow bandwidth or with transmission zeros to improve the selectivity, irises between resonators may be used (Fig. 1). The irises control the couplings which could be magnetic or electric. Some experimental results of slot coupling between 90° combline resonators are shown in [7]. However, there are no accurate modeling of the coupling in the literature.

Modeling slot coupling of combline resonators can be achieved by solving the problem of conducting posts in rectangular waveguides. Although, extensive research work has been published on this subject [8]–[12] using different methods over the past few decades, the results are not suitable for the posts in evanescent mode waveguides which is the case of combline filters. Most of the previous work is based on the assumption that TE_{10} mode is a propagating mode in the rectangular waveguide. On the other hand, for slot coupled combline filters and many other applications such as interdigital filters [13] and stepped-wall evanescent mode waveguide filters [14], the conducting posts are usually used in conjunction with other waveguide discontinuities such as irises and steps. In these cases, it is desired to model the posts as a key building block with its generalized scattering matrix, so that a cascading procedure using S-matrices [15], [16] can be applied to solve the complicated problems encountered in filter designs regardless whether the posts are in propagating or evanescent waveguides.

This paper applies the orthogonal expansion method [17], [18] to characterize the generalized S-matrix of a conducting post in a rectangular waveguide (Fig. 2). The convergence and accuracy of the numerical solutions are examined. For

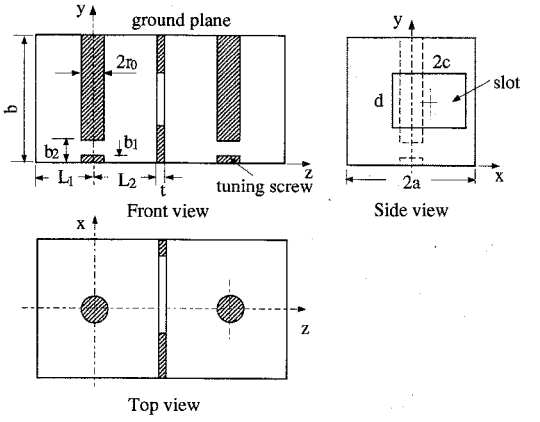

Fig. 1. Configuration of slot coupled combline resonators.

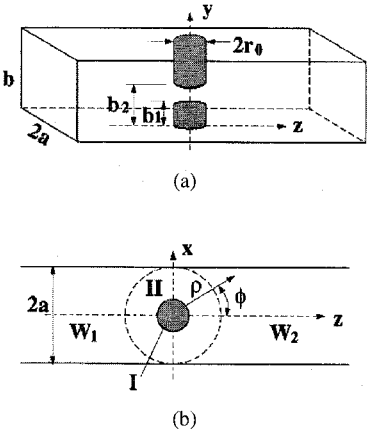

Fig. 2. Configuration of a centered post in a rectangular waveguide.

Manuscript received February 28, 1995; revised July 10, 1995. This work was supported in part by the Maryland Industrial Partnerships.

H.-W. Yao and K. A. Zaki are with the Department of Electrical Engineering, University of Maryland, College Park, MD 20742 USA.

A. E. Atia is with CTA Incorporated, 6116 Executive Blvd., Rockville, MD 20852 USA.

R. Hershtig is with K&L Microwave Inc., Salisbury, MD USA.

IEEE Log Number 9415475.

filter applications, a cascading procedure using generalized S-matrices is employed with proper terminating conditions to calculate the resonant frequencies and the slot coupling coefficients of combline cavities. Comparison between numerical and experimental results shows the validation and accuracy of this method. As an application of the modeling, a 6-pole slot coupled combline filter with finite transmission zeros and asymmetric insertion loss response is designed, built, and tested. Excellent filter response is obtained.

This method can be extended easily to the analysis and design of interdigital filters and evanescent mode waveguide filters.

II. Scattering from Conducting Posts in Rectangular Waveguides

Consider a centered conducting post in a rectangular waveguide shown in Fig. 2. By introducing an artificial cylindrical boundary at $\rho = a$, one can divide the whole structure into three regions: a cylindrical interaction region ($\rho \le a$) and two waveguide region W_1 and W_2. The cylindrical region consists of two subregions: region I ($\rho \le r_0,\ b_1 \le y \le b_2$) and region II ($r_0 < \rho \le a,\ 0 \le y \le b$). The transverse fields with respect to $\hat{\rho}$ direction in each cylindrical region can be expanded as

$$\begin{aligned}\vec{E}^s_{ct}(\rho,\phi,y) &= \sum_n \sum_j \{C^{se}_{nj} J_n(\xi^{se}_j \rho) \\ &\quad + D^{se}_{nj} Y_n(\xi^{se}_j \rho)\} \vec{e}^{\,se}_{ctnj}(\rho,\phi,y) \\ &\quad + \sum_n \sum_j \{C^{sh}_{nj} J'_n(\xi^{sh}_j \rho) \\ &\quad + D^{sh}_{nj} Y'_n(\xi^{sh}_j \rho)\} |\xi^{sh}_j| \vec{e}^{\,sh}_{ctnj}(\rho,\phi,y) \quad (1a)\end{aligned}$$

$$\begin{aligned}\vec{H}^s_{ct}(\rho,\phi,y) &= \sum_n \sum_j \{C^{se}_{nj} J'_n(\xi^{se}_j \rho) \\ &\quad + D^{se}_{nj} Y'_n(\xi^{se}_j \rho)\} |\xi^{se}_j| \vec{h}^{\,se}_{ctnj}(\rho,\phi,y) \\ &\quad + \sum_n \sum_j \{C^{sh}_{nj} J_n(\xi^{sh}_j \rho) \\ &\quad + D^{sh}_{nj} Y_n(\xi^{sh}_j \rho)\} \vec{h}^{\,sh}_{ctnj}(\rho,\phi,y) \quad (1b)\end{aligned}$$

$$\xi^{sq2}_j = k^2 - k^{sq2}_j = {k_0}^2 \epsilon_r - k^{sq2}_j \quad q = e, h \quad (2)$$

where J_n and Y_n are Bessel functions of the first kind and the second kind, respectively; $s =$ I or II; $D^{Iq}_{nj} = 0$ ($q = e$ and h). $\vec{e}^{\,sq}_{ctnj}$ and $\vec{h}^{\,sq}_{ctnj}$ represent the transverse electric and magnetic eigen fields of TE_y mode ($q = h$) or TM_y mode ($q = e$) of parallel planes bounded in y direction in the cylindrical coordinate system (ρ, ϕ, y).

For TE_y mode

$$\vec{e}^{\,sh}_{ctnj}(\rho,\phi,y) = \hat{\phi} \frac{1}{\xi^{sh2}_j} \Phi^h_n(\phi) h^{sh}_{yj}(k^{sh}_j, y) \quad (3a)$$

$$\begin{aligned}&j\omega\mu \vec{h}^{\,sh}_{ctnj}(\rho,\phi,y) \\ &= \hat{y} \Phi^h_n(\phi) h^{sh}_{yj}(k^{sh}_j, y) + \hat{\phi} \frac{1}{\xi^{sh2}_j} \frac{\partial^2}{\rho \partial\phi \partial y} \{\Phi^h_n(\phi) h^{sh}_{yj}(k^{sh}_j, y)\}\end{aligned} \quad (3b)$$

where

$$\Phi^h_n(\phi) = \begin{Bmatrix} \cos(n\phi) \\ -\sin(n\phi) \end{Bmatrix} \quad (3c)$$

$$h^{sh}_{yj}(k^{sh}_j, y) = \begin{cases} \sin(k^{Ih}_j (y - b_1)) & k^{Ih}_j = \frac{j\pi}{b_2 - b_1} \quad \text{region I} \\ \sin(k^{IIh}_j y) & k^{IIh}_j = \frac{j\pi}{b} \quad \text{region II} \end{cases} \quad (3d)$$

For TM_y mode

$$\begin{aligned}\vec{e}^{\,se}_{ctnj}(\rho,\phi,y) &= \hat{y} \Phi^e_n(\phi) e^{se}_{yj}(k^{se}_j, y) \\ &\quad + \hat{\phi} \frac{1}{\xi^{se2}_j} \frac{\partial^2}{\rho \partial\phi \partial y} \{\Phi^e_n(\phi) e^{se}_{yj}(k^{se}_j, y)\}\end{aligned} \quad (4a)$$

$$j\omega\mu \vec{h}^{\,se}_{ctnj}(\rho,\phi,y) = \hat{\phi} \frac{k^2}{\xi^{se2}_j} \Phi^e_n(\phi) e^{se}_{yj}(k^{se}_j, y) \quad (4b)$$

where

$$\Phi^e_n(\phi) = \begin{Bmatrix} \sin(n\phi) \\ \cos(n\phi) \end{Bmatrix} \quad (4c)$$

$$e^{se}_{yj}(k^{se}_j, y) = \begin{cases} \cos(k^{Ie}_j (y - b_1)) & k^{Ie}_j = \frac{j\pi}{b_2 - b_1} \quad \text{region I} \\ \cos(k^{IIe}_j y) & k^{IIe}_j = \frac{j\pi}{b} \quad \text{region II} \end{cases} \quad (4d)$$

In the waveguide regions, the transverse fields with respect to $\hat{\rho}$ direction are linear combinations of the transverse fields of waveguide eigenmodes including both forward (F) and backward (B) waves

$$\begin{Bmatrix} \vec{E}^{(1)}_{wt}(x,y,z) \\ \vec{E}^{(2)}_{wt}(x,y,z) \end{Bmatrix} = \sum_{q=e,\,h} \sum_m \sum_i \left[\begin{Bmatrix} A^{(1)q}_{mi} \\ B^{(2)q}_{mi} \end{Bmatrix} \vec{e}^{\,qF}_{wtmi} + \begin{Bmatrix} B^{(1)q}_{mi} \\ A^{(2)q}_{mi} \end{Bmatrix} \vec{e}^{\,qB}_{wtmi} \right] \quad (5a)$$

$$\begin{Bmatrix} \vec{H}^{(1)}_{wt}(x,y,z) \\ \vec{H}^{(2)}_{wt}(x,y,z) \end{Bmatrix} = \sum_{q=e,\,h} \sum_m \sum_i \left[\begin{Bmatrix} A^{(1)q}_{mi} \\ B^{(2)q}_{mi} \end{Bmatrix} \vec{h}^{\,qF}_{wtmi} - \begin{Bmatrix} B^{(1)q}_{mi} \\ A^{(2)q}_{mi} \end{Bmatrix} \vec{h}^{\,qB}_{wtmi} \right] \quad (5b)$$

where $q = e$ and h represent TM and TE modes in the waveguide, respectively. The transverse fields of an eigenmode are given by

$$\begin{Bmatrix} \vec{e}^{\,qF}_{wtmi} \\ \vec{e}^{\,qB}_{wtmi} \end{Bmatrix} = \left[\hat{y} e^q_{wymi} + \hat{\phi}(e^q_{wxmi} \cos\phi \mp e^q_{wzmi} \sin\phi)\right] \cdot \exp^{\mp\gamma_{mi} z} \quad (6a)$$

$$\begin{Bmatrix} \vec{h}^{\,qF}_{wtmi} \\ \vec{h}^{\,qB}_{wtmi} \end{Bmatrix} = \pm\left[\hat{y} h^q_{wymi} + \hat{\phi}(h^q_{wxmi} \cos\phi \mp h^q_{wzmi} \sin\phi)\right] \cdot \exp^{\mp\gamma_{mi} z} \quad (6b)$$

where

$$e^q_{wzmi}(x,y) = \begin{cases} \sin(k_{xm}(x + a)) \sin(k_{yi} y) & q = e \\ 0 & q = h \end{cases} \quad (7a)$$

$$h^q_{wzmi}(x,y) = \begin{cases} 0 & q = e \\ \cos(k_{xm}(x + a)) \cos(k_{yi} y) & q = h \end{cases} \quad (7b)$$

$${\gamma_{mi}}^2 = {k_{xm}}^2 + {k_{yi}}^2 - {k_0}^2 \epsilon_r; \quad k_{xm} = \frac{m\pi}{2a}; \quad k_{yi} = \frac{i\pi}{b}. \quad (7c)$$

The other components of the fields can be found from the z-components.

To solve the scattering from the posts, the boundary conditions have to be satisfied across two cylindrical boundaries $\rho = r_0$ and $\rho = a$. Enforcing the continuity of the tangential fields at boundary $\rho = r_0$ and properly defining the inner products, one can readily obtain a matrix equation with the following form

$$[[M_C^{\rm II}] \quad [M_D^{\rm II}]] \begin{bmatrix} \mathbf{C}^{\rm II} \\ \mathbf{D}^{\rm II} \end{bmatrix} = 0 \tag{8}$$

$\mathbf{C}^{\rm II}$ and $\mathbf{D}^{\rm II}$ are field coefficient vectors with element $C_{nj}^{{\rm II}q}$ and $D_{nj}^{{\rm II}q}$ $(q = e, h)$, respectively. $[M_C^{\rm II}]$ and $[M_D^{\rm II}]$ are diagonal block matrices of size $N^{\rm II} \times N^{\rm II}$, where $N^{\rm II}$ is the total number of eigenmodes used in cylindrical region II. Each block matrix corresponds to the inner products of the eigenmodes with same ϕ variations. Since both region I and region II are cylindrical regions, mode orthogonality can be applied and all the inner products can be obtained analytically.

At the artificial boundary $\rho = a$, the field continuity requires

$$\vec{E}_{ct}^{\rm II}(a, \phi, y) = \delta_w^{(1)}(\phi)\vec{E}_{wt}^{(1)}(x, y, z) + \delta_w^{(2)}(\phi)\vec{E}_{wt}^{(2)}(x, y, z) \tag{9a}$$

$$\vec{H}_{ct}^{\rm II}(a, \phi, y) = \delta_w^{(1)}(\phi)\vec{H}_{wt}^{(1)}(x, y, z) + \delta_w^{(2)}(\phi)\vec{H}_{wt}^{(2)}(x, y, z) \tag{9b}$$

where

$$\delta_w^{(1)} = \begin{cases} 1 & \frac{\pi}{2} < \phi \le \frac{3}{2}\pi \\ 0 & -\frac{\pi}{2} < \phi \le \frac{\pi}{2} \end{cases}, \qquad \delta_w^{(2)} = \begin{cases} 0 & \frac{\pi}{2} < \phi \le \frac{3}{2}\pi \\ 1 & -\frac{\pi}{2} < \phi \le \frac{\pi}{2} \end{cases}. \tag{10}$$

Taking cross inner product to (9a) and (9b) with $\vec{h}_{ctnj}^{{\rm II}q}$ and $\vec{e}_{ctnj}^{{\rm II}q}$, respectively, one can acquire

$$\begin{aligned} &[[\lambda_E^C] \quad [\lambda_E^D]] \begin{bmatrix} \mathbf{C}^{\rm II} \\ \mathbf{D}^{\rm II} \end{bmatrix} \\ &\quad = [[M^{(1)F}] \quad [M^{(2)B}]] \begin{bmatrix} \mathbf{A}^{(1)} \\ \mathbf{A}^{(2)} \end{bmatrix} \\ &\qquad + [[M^{(1)B}] \quad [M^{(2)F}]] \begin{bmatrix} \mathbf{B}^{(1)} \\ \mathbf{B}^{(2)} \end{bmatrix} \end{aligned} \tag{11a}$$

$$\begin{aligned} &[[\lambda_H^C] \quad [\lambda_H^D]] \begin{bmatrix} \mathbf{C}^{\rm II} \\ \mathbf{D}^{\rm II} \end{bmatrix} \\ &\quad = [[T^{(1)F}] \quad [T^{(2)B}]] \begin{bmatrix} \mathbf{A}^{(1)} \\ \mathbf{A}^{(2)} \end{bmatrix} \\ &\qquad + [[T^{(1)B}] \quad [T^{(2)F}]] \begin{bmatrix} c\mathbf{B}^{(1)} \\ \mathbf{B}^{(2)} \end{bmatrix}. \end{aligned} \tag{11b}$$

Where $\mathbf{A}^{(\ell)}$ and $\mathbf{B}^{(\ell)}$ are vectors with elements of $A_{mi}^{(\ell)q}$ and $B_{mi}^{(\ell)q}$ $(\ell = 1, 2;\ q = e, h)$, respectively. $[\lambda]$'s are diagonal matrices of size $N^{\rm II} \times N^{\rm II}$ with elements determined by the self inner products in region II. $[M^{(\ell)}]$'s and $[T^{(\ell)}]$'s are sparse matrices of size $N^{\rm II} \times N^{(\ell)}$ where $N^{(\ell)}$ is the total number of modes used in waveguide region ℓ $(\ell = 1, 2)$. The nonzero elements of the matrices are determined by the mutual inner products between the eigenmodes with the same y-variations in the waveguide regions and region II. The mutual inner products contain integrations of the following forms

$$I = \int_{-\frac{\pi}{2}}^{\frac{\pi}{2}} \exp^{\pm\gamma_{mi}z} \begin{Bmatrix} \cos(\frac{m\pi}{2a}(x+a)) \\ \sin(\frac{m\pi}{2a}(x+a)) \end{Bmatrix} \begin{Bmatrix} \cos(n\phi) \\ \sin(n\phi) \end{Bmatrix} d\phi. \tag{12}$$

To evaluate the integrations efficiently and accurately, the Bessel-Fourier orthogonal expansions [17], [18] can be applied.

Once the inner products are calculated, one may obtain the following equations from (11)

$$\begin{aligned} \begin{bmatrix} \mathbf{C}^{\rm II} \\ \mathbf{D}^{\rm II} \end{bmatrix} &= \begin{bmatrix} [M_C^{1F}] & [M_C^{2B}] \\ [M_D^{1F}] & [M_D^{2B}] \end{bmatrix} \begin{bmatrix} \mathbf{A}^{(1)} \\ \mathbf{A}^{(2)} \end{bmatrix} \\ &\quad + \begin{bmatrix} [M_C^{1B}] & [M_C^{2F}] \\ [M_D^{1B}] & [M_D^{2F}] \end{bmatrix} \begin{bmatrix} \mathbf{B}^{(1)} \\ \mathbf{B}^{(2)} \end{bmatrix} \end{aligned} \tag{13}$$

$$\begin{aligned} [M_C^{pV}] &= \{[\lambda_E^D]^{-1}[\lambda_E^C] - [\lambda_H^D]^{-1}[\lambda_H^C]\}^{-1} \\ &\quad \times \{[\lambda_E^D]^{-1}[M^{(p)V}] - [\lambda_H^D]^{-1}[T^{(p)V}]\} \end{aligned} \tag{14a}$$

$$\begin{aligned} [M_D^{pV}] &= \{[\lambda_E^C]^{-1}[\lambda_E^D] - [\lambda_H^C]^{-1}[\lambda_H^D]\}^{-1} \\ &\quad \times \{[\lambda_E^C]^{-1}[M^{(p)V}] - [\lambda_H^C]^{-1}[T^{(p)V}]\} \end{aligned} \tag{14b}$$

where $p = 1, 2$ and $V = F, B$.

The generalized scattering matrix $[S^P]$ of a cylindrical post in a rectangular waveguide can be finally obtained from (8) and (13)

$$\begin{bmatrix} \mathbf{B}^{(1)} \\ \mathbf{B}^{(2)} \end{bmatrix} = [S^P] \begin{bmatrix} \mathbf{A}^{(1)} \\ \mathbf{A}^{(2)} \end{bmatrix} = \begin{bmatrix} [S_{11}^P] & [S_{12}^P] \\ [S_{21}^P] & [S_{22}^P] \end{bmatrix} \begin{bmatrix} \mathbf{A}^{(1)} \\ \mathbf{A}^{(2)} \end{bmatrix}. \tag{15}$$

For self consistency, the numbers of eigenmodes used in the waveguide regions and cylindrical region II have to be selected to meet the following two conditions: 1) the number of modes in region II equals to the sum of those in waveguide regions W_1 and W_2, that is $N^{\rm II} = N^{(1)} + N^{(2)}$; 2) the number of the modes with same y-variations in region II equal to those in the waveguide regions.

A computer program has been developed to calculate the S-matrix of conducting posts in rectangular waveguides. Fig. 3

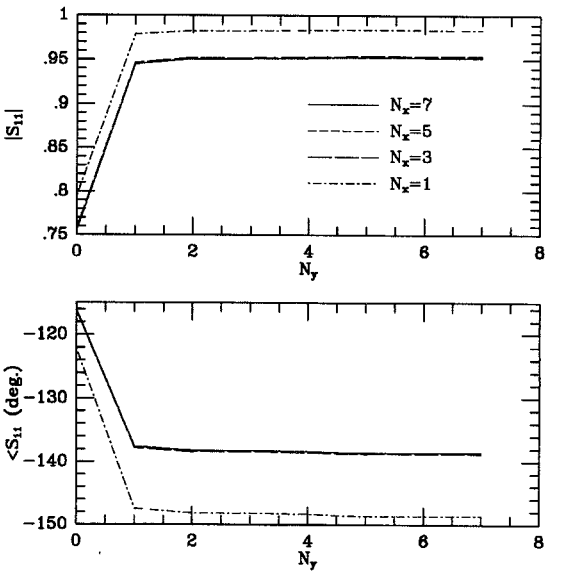

Fig. 3. Convergence of S-parameters of a metal post in a propagating waveguide with different number of modes used. $2a = 0.9''$, $b = 0.4''$, $b_1 = 0$, $b_2 = 0.1''$, $r_0 = 0.125''$, and $f = 10$ GHz.

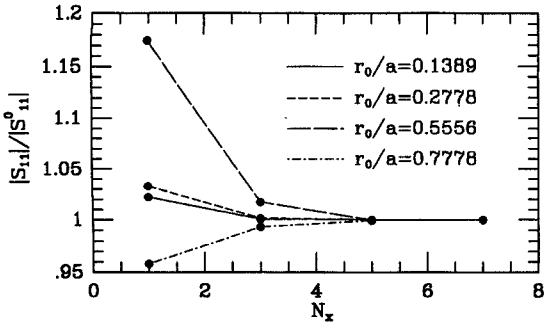

Fig. 4. Convergence of S-parameters of a metal post in a propagating waveguide with different radius of post. Dimensions same as those in Fig. 3. $N_y = 6$.

TABLE I
COMPARISON OF NUMERICAL RESULTS OF S-PARAMETERS OF A POST WITH EXPERIMENT

	Numerical		Experimental [8]	
b_2	S_{11}	S_{21}	S_{11}	S_{21}
0.024	0.99774∠-142.593	0.06721∠-52.593	0.99743∠-142.494	0.07163∠-52.494
0.048	0.98889∠-141.170	0.14867∠-51.170	0.98865∠-141.141	0.15022∠-51.141
0.100	0.95290∠-138.527	0.30328∠-48.527	0.95253∠-138.445	0.30445∠-48.445
0.1992	0.76717∠-126.016	0.64382∠-36.016	0.75403∠-125.142	0.65684∠-35.142
0.300	0.31647∠-102.157	0.94860∠-12.157	0.30978∠-101.635	0.95081∠-11.635

2a=0.9", b=0.4", b_1=0.0, r_0=0.125", f=10 GHz, Nx=5, Ny=6

presents the convergence of the dominant mode S-parameters of posts in a propagating waveguide varying the numbers of the modes used in the waveguide, where N_x and N_y are the mode index numbers in x-direction and y-direction in the waveguide, respectively. The convergence with different radii of the posts is shown in Fig. 4, where S^0_{11} represents the reflection obtained under the conditions of $N_x = 7$ and $N_y = 6$. It can be seen that even for a thick post, $N_x = 5$ and $N_y = 6$ are sufficient for the dominant mode S-parameters of posts in a propagating waveguide. However, for posts in evanescent mode waveguides, a larger N_y is required to ensure convergent results. A comparison of the numerical results of the dominant mode S-parameters of a post with the experimental results given in [8] is presented in Table I showing excellent agreement.

III. APPLICATIONS TO SLOT COUPLED COMBLINE FILTERS

A. Computation of Slot Coupling

The two slot-coupled combline resonators shown in Fig. 1 can be considered as a cascaded structure. The S-matrix network representation of the structure is given in Fig. 5, where $[S^P]$ and $[S^{P'}]$ are generalized scattering matrices of the first and the second resonators, respectively, $[S^D]$ represents the scattering matrix of the slot which can be readily obtained by full wave mode matching method [19]. With the knowledge of $[S^P]$, $[S^{P'}]$, and $[S^D]$, a cascading procedure using S-matrices [15], [16] may be employed to obtain the eigen equations for the resonant frequencies of two slot-coupled combline cavities. When the two coupled cavities are identical,

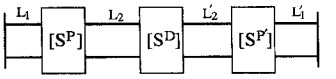

Fig. 5. S-matrix network representation of slot coupled combline resonators.

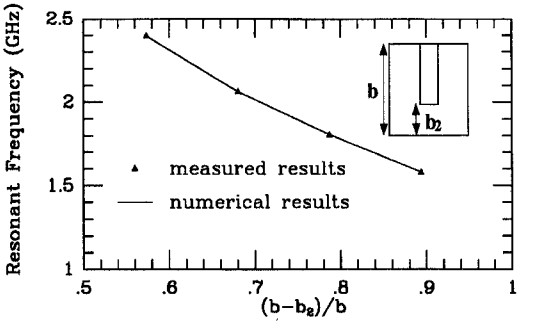

Fig. 6. Resonant frequency of a combline cavity with $2a = 0.872''$, $b = 1.872''$, $r_0 = 0.13''$, $L_1 = L_2 = 0.5''$, and $b_1 = 0.0$.

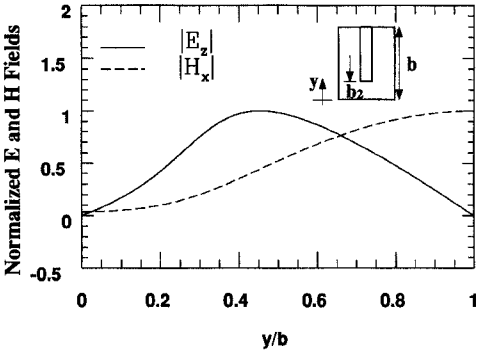

Fig. 7. Field distributions along y at the end wall of a combline cavity with 80° rod length, the other dimensions same as that in Fig. 6.

PEC and PMC may be used at the symmetrical plane to simplify the coupling computation [20]. Otherwise, a short and an open circuit conditions have to be realized at one end of the network successively to obtain two zeros (f_{z1} and f_{z2}) and one pole (f_p) of the transfer function, respectively, from which the coupling coefficient can be computed as

$$k^2 = 1 - \frac{{f_1}^2 + {f_p}^2}{{f_{z1}}^2 + {f_{z2}}^2} \tag{16a}$$

$${f_1}^2 = \frac{{f_p}^2 {f_{z1}}^2 {f_{z2}}^2}{{f_p}^2({f_{z1}}^2 + {f_{z2}}^2) - {f_{z1}}^2 {f_{z2}}^2}. \tag{16b}$$

Fig. 6 gives the numerical and experimental results of the resonant frequencies of a single combline cavity as a function of the length of the metal rod. Fig. 7 presents the field distributions along y direction at the center of one end wall of a cavity, which qualitatively indicates where a slot should be located in order to have electric or magnetic coupling. Fig. 8 gives the coupling coefficients of a slot between two identical combline cavities. Both magnetic and electric couplings are obtained by changing the dimensions of the slot, but the maximum value of electric coupling is limited. Similar result was shown experimentally in reference [7]. To obtain electric coupling, the length of the metal rod has to be greater than 45° and the slot has to be placed at the open side of the

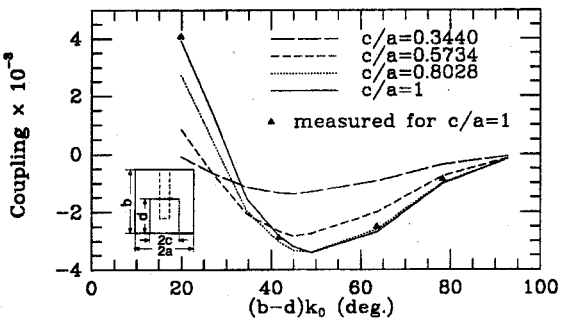

Fig. 8. Slot coupling of two identical combline cavities with slot thickness = $0.052''$, $b_2 = 0.798''$, the other dimensions same as that in Fig. 6.

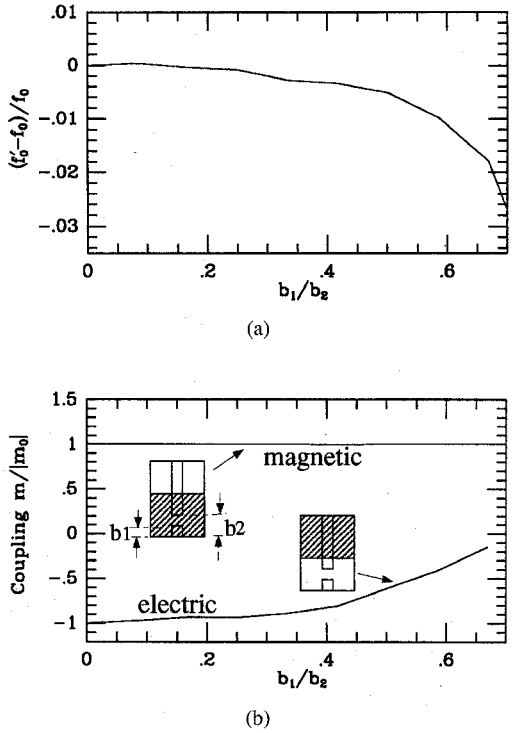

Fig. 9. Effect of tune screw on (a) resonant frequency, and (b) slot coupling of electric and magnetic types. $2a = 0.872''$, $b = 1.87''$, $r_0 = 0.13''$, $L_1 = L_2 = 0.5''$, $b_2 = 0.598''$; with slot dimensions $t = 0.052''$, $2c = 0.872''$, and $d = 1.0''$.

rod. Numerical results also show that the electric coupling and resonant frequencies are more sensitive to the tuning screw depth (b_1) than the magnetic coupling. This frequency dependent behavior of different couplings is shown in Fig. 9. In this figure, f_0 and m_0 represent the resonant frequency and the slot coupling without the tuning screw (i.e., $b_1 = 0$).

B. Design and Realization of Slot Coupled Combline Filter

As an application of the modeling, a 6-pole slot coupled combline filter centered at 915 MHz with 28 MHz bandwidth is designed. The filter is required to meet the specifications for a base station mobile communication network of 30 dB rejections beyond 890 MHz and 930 MHz. By applying the synthesis procedure introduced in [21] in conjunction with optimization, the following coupling matrix to be realized is

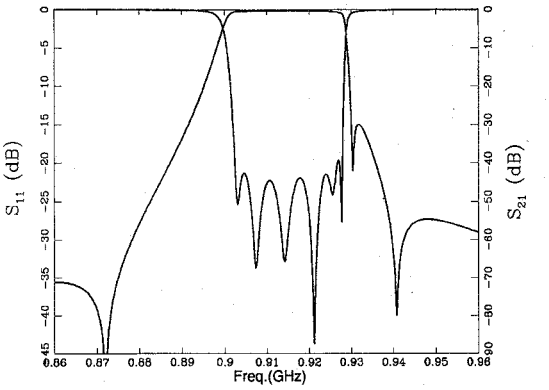

Fig. 10. Ideal response of the designed 6-pole filter.

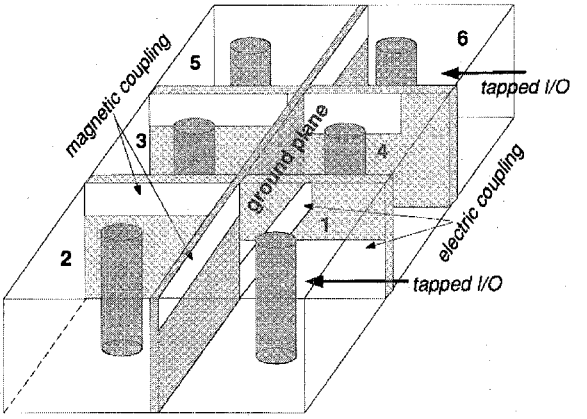

Fig. 11. Schematic configuration of the 6-pole filter realized by slot coupled combline cavities.

obtained

$$M = \begin{bmatrix} 0.025 & 0.773 & 0.0 & -0.12 & 0.0 & 0.0 \\ 0.773 & 0.0 & 0.536 & 0.0 & 0.0 & 0.0 \\ 0.0 & 0.536 & -0.03 & -0.042 & 0.528 & 0.0 \\ -0.12 & 0.0 & -0.042 & 1.007 & 0.0 & 0.210 \\ 0.0 & 0.0 & 0.528 & 0.0 & 0.0 & 0.767 \\ 0.0 & 0.0 & 0.0 & 0.21 & 0.767 & 0.075 \end{bmatrix}$$

$$R_1 = 0.949, \quad R_6 = 1.002.$$

The ideal response of the designed filter is given in Fig. 10.

The realization of the designed coupling matrix by combline cavities is achieved by the schematic configuration shown in Fig. 11, where cavity 1, 2, 3, 5, and 6 form a Tchebyscheff filter, and cavity 4 is used to provide the transmission zeros at both sides of the pass band. The lengths of resonator rods are selected around 80° to ensure enough electric couplings. The slot dimensions are determined by the method described in the last section to give the required couplings for each slot. Since the modeling does not include the interactions between slots, fine tuning of the slot dimensions is needed to minimize the return loss in the pass band. The designed filter is built and tested. The measured response of the filter is shown in Fig. 12. Fig. 13 presents the measured Tchebyscheff response of the filter when cavity 4 is detuned completely.

Comparing the ideal response in Fig. 10 with the measured response in Fig. 12, it is observed that the transmission zero

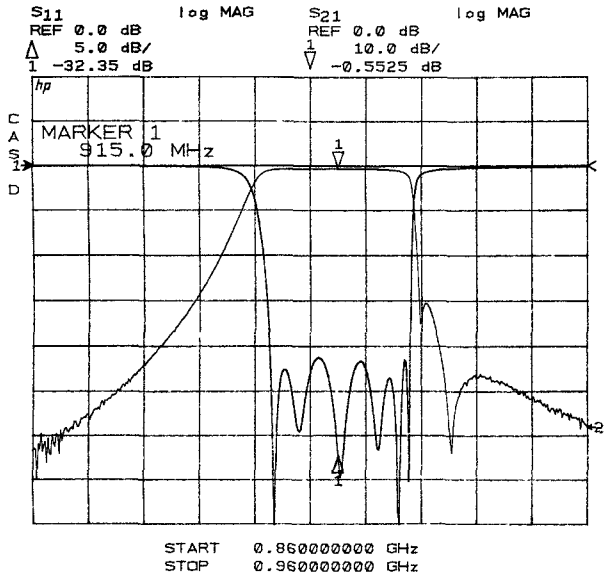

Fig. 12. Measured response of the 6-pole filter.

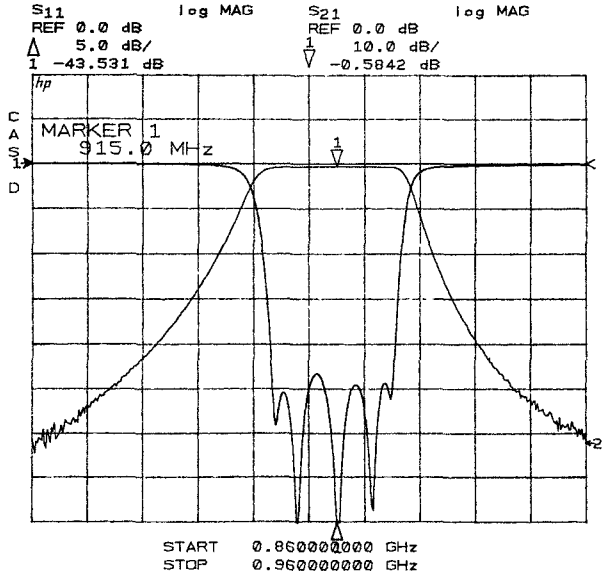

Fig. 13. Measured Tchebyscheff response of the filter when cavity 4 is detuned.

at the low side of the pass band of the measured response moves to lower frequency. The reason may be the dispersion of combline resonators.

IV. Conclusion

A rigorous method for computing the generalized scattering matrix of conducting posts in rectangular waveguides is presented. By cascading the generalized scattering matrix, slot couplings between combline cavities are computed. Numerical results for both resonant frequency and coupling coefficient agree well with experiment. It is shown that both electric and magnetic couplings can be obtained, and since the electric coupling slot is adjacent to the tuning screw, the electric coupling is more sensitive to the tuning screw than magnetic coupling. A 6-pole slot coupled combline filter with asymmetrical transmission zeros is designed and built. Excellent filter responses are obtained.

The modeling methods can be easily applied to analyze the interdigital filters, the evanescent mode series coupled waveguide filters, and waveguide filters using inductive posts.

References

[1] G. L. Matthaei, "Combline band-pass filters of narrow or moderate bandwidth," *Microwave J.*, vol. 6, pp. 82–91, Aug. 1963.
[2] E. G. Cristal, "Coupled circular cylindrical rods between parallel ground planes," *IEEE Trans. Microwave Theory Tech.*, vol. MTT-12, pp. 428–439, July 1964.
[3] J. D. Rhodes, "The stepped digital elliptic filter," *IEEE Trans. Microwave Theory Tech.*, vol. MTT-17, pp. 178–184, Apr. 1969.
[4] R. Levy and J. D. Rhodes, "A combline elliptic filter," *IEEE Trans. Microwave Theory Tech.*, vol. MTT-19, pp. 26–29, Jan. 1971.
[5] R. J. Wenzel, "Synthesis of combline and capacitively loaded interdigital bandpass filters of arbitrary bandwidth," *IEEE Trans. Microwave Theory Tech.*, vol. MTT-19, pp. 678–686, Aug. 1971.
[6] I. H. Zabalawi, "Design of linear phase selective combline filter," *IEEE Trans. Microwave Theory Tech.*, vol. MTT-30, pp. 1224–1228, Aug. 1982.
[7] R. M. Kurzrok, "Design of combline band-pass filters," *IEEE Trans. Microwave Theory Tech.*, vol. MTT-14, pp. 351–353, July 1966.
[8] N. Marcuvitz, *Waveguide Handbook*, M.I.T. Rad. Lab. Series, vol. 10. New York: McGraw-Hill, 1957, pp. 257–262.
[9] J. A. Bradshaw, "Scattering from a round metal post and gap," *IEEE Trans. Microwave Theory Tech.*, vol. MTT-21, pp. 313–322, May 1973.
[10] A. G. Williamson, "Analysis and modeling of a single-post waveguide mounting structure," *Proc. Inst. Elec. Eng.*, Oct. 1982, vol. 129, Part H, pp. 271–277.
[11] Y. Leviatan, P. G. Li, A. T. Adams, and J. Perini, "Single-post inductive obstacles in rectangular waveguide," *IEEE Trans. Microwave Theory Tech.*, vol. MTT-31, pp. 806–812, Oct. 1983.
[12] V. M. Butorin and A. T. Fialkovskii, "The theory of a resonant structure in the form of a disk located inside a rectangular waveguide between a dielectric washer and a vertical rod," *Radio Eng. & Elect. Physics*, vol. 26, pp. 22–29, Nov. 1981.
[13] G. L. Matthaei, "Interdigital band-pass filter," *IRE Trans. Microwave Theory Tech.*, vol. MTT-10, pp. 479–491, Nov. 1962.
[14] R. V. Snyder, "Broadband waveguide or coaxial filters with wide stopbands, using a stepped-wall evanescent mode approach," *Microwave J.*, vol. 26, pp. 83–88, Dec. 1983.
[15] Y.-C. Shih, T. Itoh, and L. Q. Bui, "Computer-aided design of millimeter-wave E-plane filters," *IEEE Trans. Microwave Theory Tech.*, vol. MTT-31, pp. 135–142, Feb. 1983.
[16] A. S. Omar and K. Schünemann, "Transmission matrix representation of finline discontinuities," *IEEE Trans. Microwave Theory Tech.*, vol. MTT-33, pp. 765–770, Sept. 1985.
[17] R. Gesche and N. Löchel, "Scattering by a lossy dielectric cylinder in a rectangular waveguide," *IEEE Trans. Microwave Theory Tech.*, vol. 36, pp. 137–144, Jan. 1988.
[18] X.-P. Liang and K. A. Zaki, "Modeling of cylindrical dielectric resonators in rectangular waveguides and cavities," *IEEE Trans. Microwave Theory Tech.*, vol. 41, pp. 2174–2181, Dec. 1993.
[19] H.-C. Chang and K. A. Zaki, "Evanescent-mode coupling of dual mode rectangular waveguide filters," *IEEE Trans. Microwave Theory Tech.*, vol. 39, pp. 1307–1312, Aug. 1991.
[20] H.-W. Yao, J.-F. Liang, and K. A. Zaki, "Accuracy of coupling computations and its application to DR filter design," in *IEEE MTT-S, Int. Microwave Symp. Dig.*, San Diego, 1994, pp. 723–726.
[21] A. E. Atia and A. E. Williams, "Narrow-bandpass waveguide filters," *IEEE Trans. Microwave Theory Tech.*, vol. MTT-20, pp. 258–265, Apr. 1972.

Hui-Wen Yao (S'92), for a photograph and biography, see this issue, p. 2811.

Kawthar A. Zaki (SM'85-F'91), for a photograph and biography, see this issue, p. 2811.

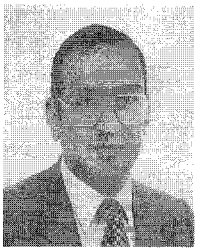

Ali E. Atia (S'67–M'69–SM'78–F'87) received the B.S. degree from Ain Shams University, Cairo, Egypt, in 1962, and the M.S. and Ph.D. degrees from the Univerity of California, Berkeley, in 1966 and 1969, respectively, all in electrical engineering.

Prior to joining COMSAT in 1969, he held various research and teaching positions at both these universities. As a Senior Scientist in the Microwave Laboratory at COMSAT Laboratories, he has made original contributions to satellite transponder and antenna technologies, most notably the development of the dual-mode microwave filters technology. He has also made significant contributions to several satellite programs, including INTELSAT IV-A, V, V-A, VI, ARABSAT, and AUSSAT. He was responsible for the design, implementation, qualification, and testing of major subsystems in COMSAT's NASA ATS-F propagation experiment and COMSTAR Ka-band beacon experiment. As Senior Director in COMSAT Systems Division he was responsible for communications systems design, integration, implementation, and testing under contracts with various government and commercial customers. From 1989 till 1994 he served as Vice President and Chief Engineer for COMSAT Technology Services. In 1994 he joined CTA Incorporated in Rockville, MD as President of its wholly owned subsidiary CTA International.

Dr. Atia is an Associate Fellow of the AIAA and a Member of Sigma Xi.

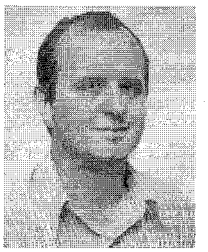

Rafi Hershtig received in 1985 the B.S. degree in electrical engineering from the Ben-gurion University in Beer-sheva, Israel. From 1985 to 1989 he worked for the microwave department of ELTA. His work focused on the development of Switched filter banks and Switched multiplexers.

In 1989 he joint K&L Microwave to work on the developing of filter based sub-systems. Since 1992 he has worked toward research and design of new product lines such as printed filters in s.s.s form and dielectric resonator filters for the commercial market place. Currently he is involved with the wireless application group, designing high "Q" elliptic response filter.